the supernatant on ice with TALON resin (Clontech). All spectra were measured on purified proteins with a LS50B Luminescence Spectrometer (Perkin-Elmer).
5. R. Y. Tsien, *Annu. Rev. Biochem.* **67**, 509 (1998).
6. H. Niwa *et al.*, *Proc. Natl. Acad. Sci. U.S.A* **93**, 13617 (1996).
7. M. Ormo *et al.*, *Science* **273**, 1392 (1996).
8. F. Yang, L. G. Moss, G. N. Phillips Jr., *Nature Biotechnol.* **14**, 1246 (1996).
9. T. Ehrig, D. J. O'Kane, F. G. Prendergast, *FEBS Lett.* **367**, 163 (1995).
10. R. Heim, D. C. Prasher, R. Y. Tsien, *Proc. Natl. Acad. Sci. U.S.A* **91**, 12501 (1994).
11. R. Heim, A. B. Cubitt, R. Y. Tsien, *Nature* **373**, 663 (1995).
12. S. Delagrave, R. E. Hawtin, C. M. Silva, M. M. Yang, D. C. Youvan, *Biotechnology* **13**, 151 (1995).
13. The cDNA fragments coding for wild-type drFP583 and the E5 mutant were subcloned into pTRE2 vector (Clontech). The HEK 293 Tet-On or 293 Tet-Off cells (Clontech) were transiently transfected with a CalPhos kit (Clontech). Doxycycline at a final concentration of 2 g/ml was added after 24 or 48 hours for Tet-On or Tet-Off cells, respectively. Cells were analyzed by FACS Calibur (Becton Dickinson). The images were taken with a XF35 Omega filter set, using a cooled charge-coupled device camera and analyzed with MetaMorph Software (Universal Imaging).
14. D. Jones, D. K. Dizon, R. W. Graham, E. P. M. Candido, *DNA* **8**, 481 (1989).
15. An E5 cDNA was subcloned into pPD49.83 vector, which contains the *hsp16-41* promoter and a 3′ UTR derived from the *unc-54* gene. Germ line transformants were obtained by microinjection of a mixture of DNA containing the [*hsp-E5*(+)] transgene (100 μg/ml) and the *unc-29*(+) gene (F35D3, 100 μg/ml) into *unc-29*(*e1072*) mutant animals. Animals were heat-shocked by floating an agar plate containing the worms in a water bath preheated to 33°C. The images were taken with a Chroma Polycroich beamsplitter 86100bs filter set [for 4′,6′-diamidino-2-phenylindole, fluorescein isothiocyanate (FITC), and *R*-phycoerythrin (PE)] and analyzed with MetaMorph Software (Universal Imaging).
16. A. Terskikh *et al.*, data not shown.
17. P. G. Okkema, S. W. Harrison, V. Plunger, A. Aryana, A. Fire, *Genetics* **135**, 383 (1993).
18. B. Galliot, D. Miller, *Trends Genet.* **16**, 1 (2000).
19. G. V. Ermakova *et al.*, *Development* **126**, 4513 (1999).
20. Plasmids containing the E5 mutant under the control of the *Otx-2* and *Xanf-1* promoters were made as previously described (*2*). The fluorescence of the E5 mutant in *Xenopus* was visualized by FITC filter set B1 of the Polyvar photomicroscope (Reihert-Jung).
21. L. D. Etkin, B. Pearman, *Development* **99**, 15 (1987).
22. A. G. Zaraisky *et al.*, *Development* **121**, 3839 (1995).
23. We thank S. Cenk, G. Davis, L. Ding, and T. Duong for technical help; E. Boncinelli and A. V. Belyavsky for the *Otx-2* and *Xanf-1* promoters; and J. Remington, R. Tsein, and M. Davis for critical reading of the manuscript. Partially supported by grants from CRDF (no. RB1-2034) and FIRCA (no. 1 RO3 TW01362-01) to A.G.Z.

27 April 2000; accepted 17 October 2000

Oxygen Activation and Reduction in Respiration: Involvement of Redox-Active Tyrosine 244

Denis A. Proshlyakov,[1] Michelle A. Pressler,[1] Catherine DeMaso,[1] Joseph F. Leykam,[2] David L. DeWitt,[2] Gerald T. Babcock[1]*

Cytochrome oxidase activates and reduces O_2 to water to sustain respiration and uses the energy released to drive proton translocation and adenosine 5′-triphosphate synthesis. A key intermediate in this process, P, lies at the junction of the O_2-reducing and proton-pumping functions. We used radioactive iodide labeling followed by peptide mapping to gain insight into the structure of P. We show that the cross-linked histidine 240–tyrosine 244 (His^{240}-Tyr^{244}) species is redox active in P formation, which establishes its structure as Fe^{IV}=O/Cu_B^{2+}-H^{240}-Y^{244}•. Thus, energy transfer from O_2 to the protein moiety is used as a strategy to avoid toxic intermediates and to control energy utilization in subsequent proton-pumping events.

Respiration activates and reduces 95% of the O_2 that we consume. In this process, the terminal respiratory enzyme, cytochrome oxidase, couples exergonic dioxygen reduction to endergonic proton translocation to drive adenosine 5′-triphosphate synthesis. There is now a relatively good understanding of the cytochrome oxidase reaction cycle (*1*) in which O_2 binds and is eventually reduced to water (Fig. 1). However, the structure of a key intermediate, **P**, which lies at the intersection of the O_2 reduction phase and the proton translocation function, has not been determined. The major uncertainty pertains to the location of one of its strongly oxidizing equivalents, the reduction of which drives the initial events in proton pumping. Reduction of **P** involves at least two proton-controlled, one-electron reduction steps, **P**→**F** (ferryl oxo species) and **F**→**O** (ferric hydroxo species) (*2*), each of which conserves appreciable energy in the chemiosmotic gradient (*3*), although the details are controversial (*4*–*7*).

Spectroscopic analysis shows that **P** is a bond-cleaved Fe^{IV}=O species (*1*, *2*). Neither heme iron nor oxygen changes its oxidation state upon the **P**→**F** transition (*8*), however, which poses the question as to the location of the extra oxidizing equivalent in **P**. Formation of a long-lived (>10 μs) heme π-cation radical can be ruled out (*1*, *2*). Recent observations of a covalent cross-link between the Cu_B ligand, H^{240}, and Y^{244} in the vicinity of heme a_3 (Fig. 1) (*9*, *10*) suggested immediately the location of this oxidizing equivalent and provided a rationale for the lack of definitive electron paramagnetic resonance radical signatures in **P** as arising from exchange coupling between Y^{244} and Cu_B (*11*). However, the experimental observations can also be explained by formation of Cu_B^{III} or by magnetic interactions between Cu_B and heme a_3, if the radical is located elsewhere. The development of protein radicals in a small fraction of **P** species under some conditions has been reported (*12*–*17*), but the identity of these species and their catalytic relevance is unclear.

Because spectroscopic techniques ap-

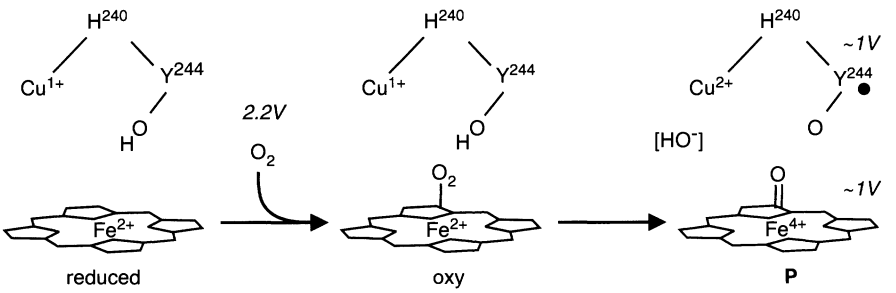

Fig. 1. Oxygen reduction and formation of **P** in the oxidative phase of the cytochrome oxidase/O_2 cycle. Only heme a_3 and the redox-active Cu_B-ligated Y^{244}-H^{240} cross-linked structure are shown. See (*11*, *33*, *34*) for details.

[1]Department of Chemistry and [2]Department of Biochemistry, Michigan State University, East Lansing, MI 48824, USA.

*To whom correspondence should be addressed. E-mail: babcock@cem.msu.edu

pear unlikely to provide an unambiguous **P** structure, chemical modification with a radical-sensitive agent, I^-, has been adopted as a probe for the presence of a radical in **P**. Iodide has been shown to label tyrosine radicals, but not neutral tyrosines, covalently (*18*). Samples of **P** (*19*) were labeled with $^{125}I^-$ (*20*), subjected to peptide mapping analysis (*21*), and compared with those of various control samples (Fig. 2). Although the absolute amount of incorporated $^{125}I^-$ is small, the observed degree of labeling is consistent with expectations (*22*). Radioactivity profiles of the resting enzyme iodinated under identical conditions were used as controls for nonspecific labeling by I_3^- or HOI, which are generated in acidic solution and react with all tyrosines. By using reversed-phase high-performance liquid chromatography (HPLC), we separated the large subunits (I to III) and hemes of $^{125}I^-$ labeled cytochrome c oxidase from minor subunits (IV to XIII) and residual free iodide (Fig. 2A). Two fractions, the heme and the binuclear center–containing subunit I, exhibited substantial increases in radioactive labeling in **P**. Some increase was observed in the minor-subunits fraction, but subsequent separation showed that most of the radioactivity was eluted in the injection volume. The heme fraction was further analyzed to identify peptides or their fragments that may be labeled in **P**, but no such peptides were found; radioactivity profiles followed closely the absorption of the heme. We conclude from these observations that only the heme and subunit I are covalently labeled by $^{125}I^-$ in **P**.

To identify the particular residue(s) labeled by iodide in **P**, we subjected subunit I to proteolysis by CNBr and separated the resulting peptides by HPLC (*21*) (Fig. 2B). Only one peptide, CB16 (L^{209}. . .M^{253}), which contains the H^{240}-Y^{244} cross-linked pair, showed a strong increase in radioactivity between **P** and the oxidized enzyme (*23*). A group of large and hydrophobic peptides eluted at later times and exhibited low levels of dispersed labeling. These larger peptides include CB15,16, and probably other partially hydrolyzed species that contain the CB16 fragment (*24*).

CB16 has two Tyr, one Trp, and several Phe residues. It was further cleaved at D-P^{222} and D-P^{228} by mild acid hydrolysis in 75% formic acid (*25*). Only one of three resulting peptides, CB16Hdr, selectively retained the radioactive label (Fig. 2**C**) (*23*). This shorter fragment was used for amino acid sequence analysis (Fig. 3). A substantial increase in the radioactivity of the eluate derived from **P** was observed at the 17th cycle, which corresponds to elution of the H^{240}-Y^{244} cross-linked dimer (*25*). No change in radioactivity was observed in the cycles corresponding to Y^{231} and W^{236}. We conclude that the only protein site labeled in **P** is the H^{240}-Y^{244} cross-linked dimer.

In the case of peroxidases, halogenation of tyrosine involves the two-electron reduction of the ferryloxo porphyrin π-cation radical species ([Por·]Fe^{IV}=O, compound I) by halide (*26*–*28*). Enzyme-bound (E-OX^-) or free (HOX; X=Cl, Br, I) species generated in this process are most likely involved in tyrosine labeling (*27*, *29*). If such a reaction were to take place in **P**, HOI would react not only with tyrosyl radicals, as I^- does, but nonspecifically with any

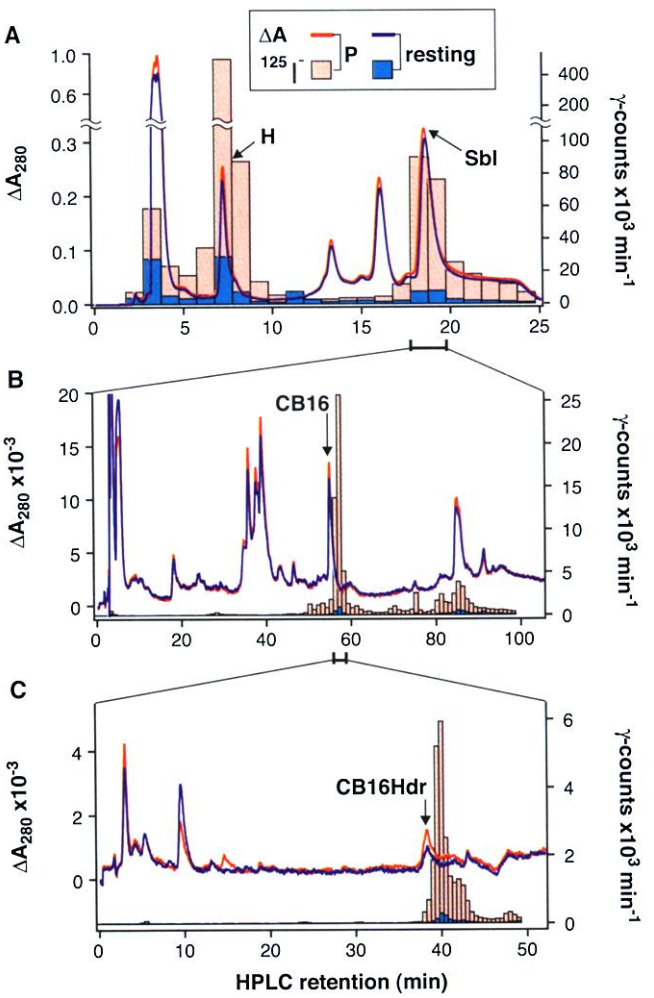

Fig. 2. Peptide mapping of the site labeled with $^{125}I^-$ in the **P** species of cytochrome oxidase. (**A**) Separation of subunit I (SbI) and the heme (H) from minor subunits. (**B**) Separation of CNBr peptides derived from subunit I. (**C**) Mild acid hydrolysis of CB16. A small amount of unhydrolyzed CB16 is seen as a shoulder after elution of CB16Hdr (*23*). Brackets below the time axis indicate fractions used in the subsequent step.

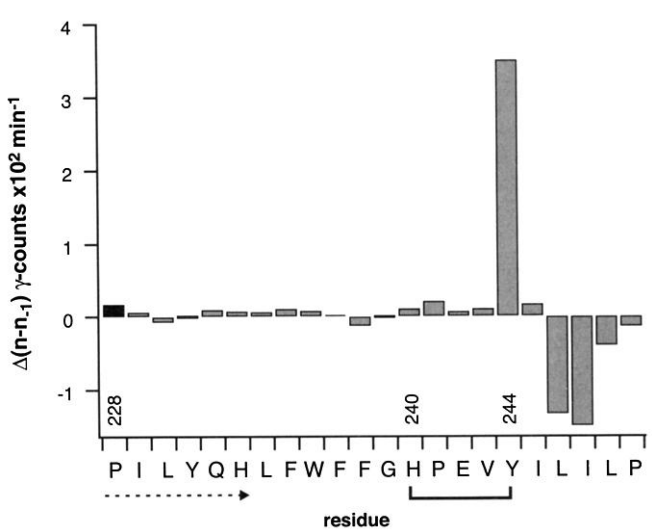

Fig. 3. Radioactivity profile along the amino acid sequence of CB16Hdr derived from iodinated **P**. Data are shown as the difference from the preceding cycle, except for the first residue, for which absolute activity is shown. The dotted arrow indicates the sequence observed for the native peptide. The location of the H^{240}-Y^{244} cross-linked structure is shown by the bracket (*25*). Abbreviations for the amino acid residues are as follows: E, Glu; F, Phe; G, Gly; H, His; I, Ile; L, Leu; P, Pro; Q, Gln; V, Val; W, Trp; and Y, Tyr.

tyrosine in the vicinity of the binuclear center (*27*). On the other hand, labeling of the heme and subunit I may represent separate instances of the specific reaction between iodide and strong, one-electron oxidizing species (*18*). To distinguish these possibilities, we carried out iodination of **F**, which contains no radical (*8*). We found that **F** exhibited heme labeling comparable to that of **P**, whereas iodination of the heme in the resting enzyme was substantially less. This ratio was reversed in the H^{240}-Y^{244} region, where **P** was specifically labeled, but **F** showed no specific labeling in comparison with the resting enzyme (*30*). The differences in iodination of the heme and the protein observed for **P** and **F** indicate that the specific increase in labeling of the H^{240}-Y^{244} structure in **P** is due to direct reaction between iodide and the radical. It is consistent with the low reactivity of the protein-radical form of peroxidases Compound I ([Por]Fe^{IV}=O R·) toward two-electron oxidation of iodide (*28*, *31*). The specific labeling of both the heme and H^{240}-Y^{244} in **P** and of the heme only in **F** also argues against involvement of a diffusible iodinating species through a peroxidase-like mechanism. The possibility of apparent labeling of **P** as a result of contamination with **F′**, another species at the same oxidation level as **P**, but spectrally identical to **F**, has been excluded based on the comparison of optical spectra and iodination pattern of the **P** and **F′** species (*32*).

The H^{240}-Y^{244} cross-linked structure is the only protein site in cytochrome oxidase that is specifically labeled by $^{125}I^-$ in **P**. This result indicates that the unusual dimer is redox active during O_2 reduction. Thus, **P** exists as a heme a_3 ferryloxo adduct with the Cu_B-ligated, H^{240}-Y^{244} cross-linked structure oxidized to a radical state (Fig. 1). It provides solid support for the mechanism of dioxygen activation by active-site hydrogen-atom abstraction (*11*), although the details of this mechanism most likely require modification (*33*, *34*). In a broader sense, our results highlight the emerging general strategy of both heme and nonheme oxygen-metabolizing enzymes (*1*). Oxygen is rapidly reduced to water in a single step, with the oxidizing equivalents generated transferred to the enzyme itself for further processing. This general strategy is flexible and efficient. Partially reduced, toxic oxygen species are avoided, and enzyme control over high-energy, but protein-localized, intermediates is facilitated. As for cytochrome oxidase, the structural definition of **P** provides the basis for analysis of subsequent events that drive the proton pumping function of the enzyme. The mechanistic basis for the unusual cross-link may be to enforce rigidity to ensure efficient proton-coupled electron transfer to substrate, as calculations (*35*) and experiments (*36*) show no appreciable change in the thermodynamic properties of the tyrosine induced by the linkage to the histidine.

References and Notes

1. G. T. Babcock, *Proc. Natl. Acad. Sci. U.S.A.* **96**, 12971 (1999).
2. T. Kitagawa, T. Ogura, *Prog. Inorg. Chem.* **45**, 431 (1997).
3. M. Wikström, *Nature* **338**, 776 (1989).
4. H. Michel, *Biochemistry* **38**, 15129 (1999).
5. ———, *Nature* **402**, 602 (1999).
6. M. I. Verkhovsky, A. Jasaitis, M. L. Verkhovskaya, J. E. Morgan, M. Wikström, *Nature* **400**, 480 (1999).
7. M. Wikström, *Biochemistry* **39**, 3515 (2000).
8. Resonance Raman studies show that both **P** and **F** have a Fe^{IV}=O structure at heme a_3, although they belong to the two- and three-electron oxidation levels, respectively. The immediate environment of the heme a_3 may differ significantly between the two species, however, as reflected in their $\nu_{Fe=O}$ frequencies. The sources of this difference, including the possible effect of Y^{244}·, have been discussed earlier (*11*).
9. S. Yoshikawa *et al.*, *Science* **280**, 1723 (1998).
10. C. Ostermeier, A. Harrenga, U. Ermler, H. Michel, *Proc. Natl. Acad. Sci. U.S.A.* **94**, 10547 (1997).
11. D. A. Proshlyakov, M. A. Pressler, G. T. Babcock, *Proc. Natl. Acad. Sci. U.S.A.* **95**, 8020 (1998).
12. G. M. Clore, L. E. Andreasson, B. Karlsson, R. Aasa, B. G. Malmstrom, *Biochem. J.* **185**, 155 (1980).
13. M. Fabian, G. Palmer, *Biochemistry* **34**, 13802 (1995).
14. F. MacMillan, A. Kannt, J. Behr, T. Prisner, H. Michel, *Biochemistry* **38**, 9179 (1999).
15. Y. R. Chen, M. R. Gunther, R. P. Mason, *J. Biol. Chem.* **274**, 3308 (1999).
16. A. Koppenhöfer, R. Little, D. J. Lowe, S. J. Ferguson, N. J. Watmough, *Biochemistry* **39**, 4028 (2000).
17. S. E. Rigby, S. Junemann, P. R. Rich, P. Heathcote, *Biochemistry* **39**, 5921 (2000).
18. Y. Takahashi, K. Satoh, *Biochim. Biophys. Acta* **973**, 138 (1989).
19. Enzyme preparation. Bovine heart cytochrome oxidase was purified as described (*11*). The enzyme was used as isolated if Na ascorbate was the reductant. If CO or H_2O_2 was used, isolation was followed by a turnover procedure that involved anaerobic reduction with Na dithionite at pH 8.8 and reoxidation by air to generate the fast enzyme. Enzyme stock solution was ~500 μM. **P** species. Two methods were used to generate **P**, both of which produced similar iodide labeling results. Method 1: Aerobic enzyme stock (40 μl) was placed under CO. Na ascorbate (2 μl) was added to yield 750 μM, and the solution was incubated and stirred overnight. **P** was generated by oxidizing the sample with 2 volumes of O_2-saturated 1.5 M urea in 3.75 mM borate buffer for 3 min on ice at pH 8.1. Method 2: CO-saturated, unbuffered 2.7 M urea solution (18 μl) was added to 30 μl of O_2-saturated fast enzyme in a microsyringe, incubated for 5 min at room temperature, and followed by 5 min of aerobic stirring on ice to remove residual CO before acidification. For the **F′** species, CO-saturated water was substituted for CO-saturated urea solution, and the concentration of urea in acidic buffer (*20*) was increased to compensate for that. **F** was generated by the addition of 13.5 μl of 32 mM H_2O_2 in water to 30 μl of enzyme stock. After 1 min, 4.5 μl of catalase (20 U/μl) was added, and the sample was incubated for 5 min on ice. For resting (fast) enzyme, the enzyme stock was diluted with water and preincubated with catalase for >1 hour.
20. Iodination. Samples (*19*) were diluted with acidic buffer, containing $^{125}I^-$ (2.5 mCi/nmol) and various concentrations of urea. The final composition was either 79 μM enzyme, 41 μM $Na^{125}I$, 1 M urea, 40 mM $Na_2S_2O_3$, and 0.5 M Na acetate buffer (pH 4.8), at 4°C, in 6 μl, or 120 μM enzyme, 90 μM $Na^{125}I$, 1 M urea, 0.6 M Na acetate buffer (pH 4.9), at 4°C, with or without 20 to 40 mM $Na_2S_2O_3$ in 4.1 μl, for samples prepared with methods 1 or 2, respectively. Iodination was carried out in closed aerobic vials in the dark for 5 to 15 min at 4°C. The reaction was terminated by dilution with 100 μl of 2.5% $ZnSO_4$ in 0.2 M Na acetate (pH 5.8), with or without 40 mM $Na_2S_2O_3$, depending on its presence in the iodination mixture. Samples were made alkaline to pH 8.5 by dilution with 1 ml of cold 17 mM borate buffer, at which point the enzyme precipitated. After centrifugation, pellets were rinsed twice with the same buffer and dissolved in 200 μl of 0.4 M Na acetate (pH 5.0) and 40 mM $Na_2S_2O_3$. This procedure was followed by repeating precipitation with 1 ml of 17 mM borate buffer and centrifugation. Samples were precipitated and rinsed three times.
21. Peptides were separated by HPLC on a 2.5 mm C4 Vydac column with a Waters 2690 separation module (Waters, Milford, MA). Fractions were analyzed with a Cobra II auto-gamma counting system (Packard Instrument, Meriden, CT). Large subunits were separated in a gradient of 55:45 MeCN:i-propanol in the presence of 60% formic acid. CNBr cleavage of subunit I was carried out at 800:1 CNBr/Met in 60% formic acid for 4 hours at room temperature. CNBr peptides were separated as described (*24*). The products of mild acid hydrolysis (*25*) were separated in a gradient of MeCN in the presence of 20% formic acid. Small subunits were separated in a gradient of MeCN in water. NH_2-terminal amino acid sequence analysis was carried out with a Perkin-Elmer model 494 analyzer (Applied Biosystems, Foster City, CA). For iodinated peptides, the eluate from each cycle of sequencing was analyzed for radioactivity without separation.
22. Cytochrome oxidase reacts with halides very slowly (*37*). Stabilization of **P** with urea and iodination at low pH allowed us to overcome this problem. The pH dependence of Cl^- binding (*37*) and our results on $^{125}I^-$ labeling at various pH values indicate that the protonated halide, rather than the bare anion, accesses the active site. Cl^- and Br^- exhibit similar kinetics of reaction with the binuclear center at pH 6.5 (*37*). From these results, a pseudo–first order reaction rate between I^- and the binuclear center of $\sim 8 \times 10^{-5}$ min^{-1} is predicted for the conditions used in this study. At this rate, an estimated $\sim 4 \times 10^{-4}$ mole fraction of **P** will react with iodide over 5 min at 22°C, which is consistent with our experimental value of $\sim 2 \times 10^{-3}$ at 4°C. The rate may be lower due to the size of iodide and the lower temperature, but accessibility is enhanced by urea (not shown).
23. A small delay between the native CB16 and CB16Hdr peptides (optical bands) and their corresponding iodinated derivatives (radioactivity) is due to the increased hydrophobicity of the latter introduced by the iodide label. Labeled peptides are not seen optically (*22*).
24. S. Hensel, G. Buse, *Biol. Chem. Hoppe Seyler* **371**, 411 (1990).
25. G. Buse, T. Soulimane, M. Dewor, H. E. Meyer, M. Bluggel, *Protein Sci.* **8**, 985 (1999).
26. R. Roman, B. Dunford, *Biochemistry* **11**, 2076 (1972).
27. W. Sun, H. B. Dunford, *Biochemistry* **32**, 1324 (1993).
28. A. Taurog, M. L. Dorris, D. R. Doerge, *Arch. Biochem. Biophys.* **330**, 24 (1996).
29. R. D. Libby, T. M. Beachy, A. K. Phipps, *J. Biol. Chem.* **271**, 21820 (1996).
30. In the presence of thiosulfate, the increase in iodination in the H^{240}-Y^{244} region in **P** relative to the resting enzyme is 20 to 30 times (Fig. 2). Thiosulfate was not used when **F** was compared with other species because it alters the optical spectrum of **F**. The absence of thiosulfate resulted in increased nonspecific labeling and an elevated background, which reduced the difference between **P** and the resting enzyme to ~2.5 times. Under these conditions, specific labeling (i.e., excess over the resting enzyme) of the heme in **F** reached 75% of that of **P**, whereas labeling of CB16Hdr in **F** remained at the level or below that of the resting enzyme and exhibited no specific labeling.
31. D. Deme, A. Virion, J. L. Michot, J. Pommier, *Arch. Biochem. Biophys.* **236**, 559 (1985).

32. When **P** is subjected to a jump from mildly alkaline pH to below pH 6.5, it converts within minutes to the **F′** species—a spectral form at the peroxy level in terms of number of oxidizing equivalents (*13*, *14*, *17*, *38*), but spectrally identical to **F** (*8*). Iodination of **P**, rather than **F′**, at acidic pH was possible by finding that exposure to moderate concentrations of urea (1 M) during formation of **P** at alkaline pH abolishes the **P**→**F′** conversion upon a subsequent acid jump [half-time ($t_{1/2}$) > 30 min)]. Stabilization was not observed when **P** was generated without urea and added to an acid buffer containing urea. Treatment with 1 M urea had no effect on the characteristic difference absorption spectra of **P**, **F**, or **F′** at pH 5 when compared with typical spectra of these forms, indicating that the structure of the binuclear center remains intact. When **P** and **F′** were iodinated under identical conditions, **F′** exhibited only a modest ~twofold increase in labeling of both the heme and subunit I. A much greater increase in labeling of **F′** is expected (>10 times) from the optical spectra of samples if the possibility of **F′** contamination as a source of peptide labeling in **P** is considered. Labeling of both the heme and subunit I in **F′** can be expected because its structure is likely to be similar to that of **P**. Location of the iodide label in **F′** is currently under investigation.

33. M. R. Blomberg, P. E. Siegbahn, G. T. Babcock, M. Wikstrom, *J. Inorg. Biochem.* **80**, 261 (2000).

34. ———, *J. Am. Chem. Soc.*, in press.

35. F. Himo, L. A. Eriksson, M. R. A. Blomberg, P. E. M. Siegbahn, *Int. J. Quantum Chem.* **76**, 714 (2000).

36. K. M. McCauley, J. M. Vrtis, J. Dupont, W. A. van der Donk, *J. Am Chem. Soc* **122**, 2403 (2000).

37. A. J. Moody, C. E. Cooper, P. R. Rich, *Biochim. Biophys. Acta* **1059**, 189 (1991).

38. A. J. Moody, P. R. Rich, *Eur. J. Biochem.* **226**, 731 (1994).

39. We thank M. I. Verkhovsky for critical and helpful discussions. Supported by NIH grants GM25480 and GM57323.

12 April 2000; accepted 25 October 2000

Control of SIV Rebound Through Structured Treatment Interruptions During Early Infection

Franco Lori,[1] Mark G. Lewis,[2] Jianqing Xu,[1] Georg Varga,[1] Donald E. Zinn Jr.,[1] Carrol Crabbs,[2] Wendeline Wagner,[2] Jack Greenhouse,[2] Peter Silvera,[2] Jake Yalley-Ogunro,[2] Carmine Tinelli,[3] Julianna Lisziewicz[1]*

In a randomized controlled trial with acute simian immunodeficiency virus (SIV)–infected macaques, both highly active antiretroviral therapy (HAART) and HAART with fixed-schedule structured treatment interruption (STI-HAART; alternating 3 weeks on and 3 weeks off therapy) suppressed viral load. In the STI-HAART group, T cell virus-specific immune response (VIR) and control of viral rebound increased concurrently during subsequent interruptions. In contrast, VIR did not increase and SIV rebounded after permanent treatment withdrawal in all animals on continuous HAART. Fixed-schedule STI-HAART appears to be an effective alternative to continuous HAART for the early treatment of retroviral infection.

The introduction of HAART represented a milestone in the treatment of HIV infection, and has been associated with a 70 to 80% decline in mortality among AIDS patients. However, virus suppression by HAART is not associated with the appearance of HIV-specific immune responses, and withdrawal of HAART is usually followed by a rapid increase in the number of viral particles in the blood, or viral rebound, and loss of CD4 T lymphocytes (*1*–*4*). Further, the long-term use of HAART is prohibitively expensive for many patients, and has been associated with toxicity and adherence problems (*5*).

STI-HAART, involving repetitive on-and-off cycles of HAART, is an attractive alternative to continuous treatment (*6*), because it might be used to enhance the utility of HAART. The initial excitement began with the description of the Berlin patient, who was able to control HIV after cycling on and off therapy twice (*7*). There is some evidence that STI-HAART can be used shortly after infection to induce immune control of viral replication (*6*–*9*), or during established infection (*10*) to reduce drug-related toxicity or to favor the reappearance of the wild-type virus (*11*). However, no well-controlled study has yet demonstrated a clear advantage of STI-HAART over HAART. Two potential strategies might be followed with STI-HAART: cycle HAART according to a fixed schedule or resume drug treatment after the virus reappears in the plasma. We evaluated a fixed-schedule STI-HAART, because it can be translated into a simple method of managing patients. We selected a symmetrical schedule, with 3 weeks on, then 3 weeks off drug treatment.

We chose to use infection of rhesus macaques by simian immunodeficiency virus (SIVmac251) as a model to compare continuous HAART with a fixed-schedule STI-HAART, because the course of that disease is analogous to that of HIV infection in humans. Seventeen rhesus macaques were infected via mucosal (intrarectal) inoculation with SIVmac251. All animals had seroconverted before treatment was initiated (6 weeks after challenge). The animals were randomized into three groups. One group (five animals) served as an untreated control. The other two groups, (six animals each) were treated for 21 weeks. One of these groups, ("continuous HAART"), was treated with (*R*)-9-(2-phosphonylmethoxypropyl) adenine (PMPA) (*12*) (20 mg/kg body weight, once daily subcutaneously), didanosine (ddI) (10 mg/kg, once daily intravenously), and hydroxyurea (HU) (*13*–*15*) (15 mg/kg, once daily intravenously). The other group ("STI-HAART") was treated with the same drugs according to a fixed schedule consisting of 3 weeks on and 3 weeks off therapy.

Plasma viremia in all three groups had reached a plateau, with an average of 200,000 to 300,000 copies/ml before treatment was started. As expected, viremia continued to increase in the untreated animals (Fig. 1). All 12 treated animals responded to therapy with a rapid decrease in plasma viremia. In the continuous HAART group, viremia became undetectable in all animals by 8 weeks of therapy. In the STI-HAART group, viremia became undetectable in four of six (4/6) animals at week 8 (during the second cycle of treatment) and in 6/6 animals at weeks 14 and 20 (during the third and fourth cycle of treatment, respectively). In both groups, viremia was significantly lower than their baseline values ($P < 0.05$) (*16*) and also significantly lower ($P < 0.01$) than that in the untreated group at all times during therapy. From week 14 of therapy until permanent withdrawal of treatment, the viremia level of the STI-HAART group was not significantly different from that of the continuous HAART group ($P = 0.8$, 0.2, and 0.8, at weeks 14, 17, and 20, respectively). In the STI-HAART group, the rate of plasma viral load rebound during the first interruption was 0.17 log/day, a statistically significant figure ($P < 0.05$), comparable to the rate of

[1]Research Institute for Genetic and Human Therapy (RIGHT), Medical-Dental Building SW307, 3900 Reservoir Road, NW, Washington, DC 20007, USA, and Pavia, Italy. [2]Southern Research Institute, Frederick, MD 21701, USA. [3]IRCCS Policlinico S. Matteo, Pavia, Italy.

*To whom correspondence should be addressed. E-mail: right@gunet.georgetown.edu